Special Collection

Synthesis and Photochemical Investigation of Tetraacylgermanes

Carola Haslinger[+],[a, b] Lukas P. Leutgeb[+],[a, b] Michael Haas,[c] Stefan Baudis,*[a, b] and Robert Liska*[b]

Tetraacylgermanes are auspicious candidates for additive manufacturing (such as lithography based ceramic manufacturing), as they are known to show high reactivity towards (meth)acrylates and absorption at wavelengths above 460 nm. We synthesized two novel tetraacylgermanes and investigated the reactivity of these compounds with methoxy groups in the *ortho* position of the aromatic moiety by comparing them both to reference substances lacking this substitution pattern and to the commercial benchmark Ivocerin®. In order to rationally assess the performance of these photoinitiators, steady-state photolysis (SSP) experiments and RT-FTIR photorheology measurements were performed. Comparable strong absorption in the long wavelength region and high photoreactivity has been found for the new initiators.

Introduction

Photopolymerization has been used for more than half a century for the curing of (meth)acrylate-based materials. It has an ever-growing range of applications: starting from the curing of protective and decorative coatings,[2] up to more advanced technologies, such as tissue engineering,[3] dental composites,[4] aerospace applications[5] or 3D printing[6] and are thus necessary materials to tackle the challenges of the 21st century. Custom made ceramic parts are sought after for microturbines, chip-manufacturing and dental implants. The solution regarding the demand for above mentioned products in combination with photopolymerization is lithography based ceramic manufacturing (LCM, displayed in Figure 1). Herein, a highly filled photopolymerizable formulation with ceramic particles is 3D-printed in a layer-by-layer fashion.

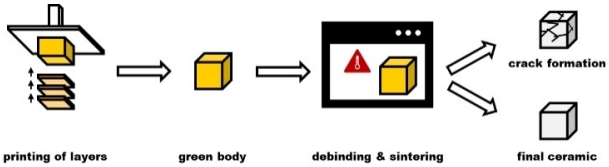

Figure 1. Schematic depiction of the LCM process.

One crucial component of a highly filled formulation with ceramic particles is the photoinitiator (PI). Light is transformed into chemical energy by generating radicals, so the polymerization can take place. As the ceramic particles are then embedded in a polymer network, the polymer is acting as binder in the manufactured green body. Thus, thermal treatment to remove residual solvent and to decompose the polymer is necessary prior to sintering.[7] However, a critical part in LCM already arises during the printing, because the layer thickness is determinative for the shaping process.[8]

The penetration depth of light into the suspension containing the polymerizable formulation with ceramic particles is of utmost importance, as it is crucial for generating sufficient layer thickness.[9] Mitterbauer *et al.*[10] proved that the depth of cure (C_d) can be enhanced by utilizing PIs with a higher absorption in the tail out region of the absorption spectrum compared to Ivocerin®. This allows the utilization of red-shifted LEDs for the printing process because longer wavelengths lead to a higher penetration depth of light.

To achieve this red shift in the absorption spectra of PIs, group 14 heteroatoms (P, Si, Ge, Sn) were introduced at the α-position next to the benzoyl chromophore. In the 1980s, acylphosphine oxides (such as diphenyl-2,4,6-trimethyl benzoyl phosphine oxide (TPO) and phenyl-bis(2,4,6-trimethyl benzoyl) phosphine oxide (BAPO)) were developed as PIs that were shown to be of great use for curing coating with TiO_2 pigments and composites.[11] This is mainly due to their absorption maxima in the near UV region with a tail-out into the visible range.

[a] C. Haslinger,[+] L. P. Leutgeb,[+] Dr. S. Baudis
Christian Doppler Laboratory for Advanced Polymers for Biomaterials and 3D Printing
Getreidemarkt 9, 1060 Vienna (Austria)
E-mail: Stefan.baudis@tuwien.ac.at
Homepage: www.baudislab.com
[b] C. Haslinger,[+] L. P. Leutgeb,[+] Dr. S. Baudis, Prof. Dr. R. Liska
Institute of Applied Synthetic Chemistry
Vienna University of Technology
Getreidemarkt 9, 1060 Vienna (Austria)
E-mail: Robert.liska@tuwien.ac.at
[c] Dr. M. Haas
Institute of Inorganic Chemistry
Graz University of Technology
Stremayrgasse 9, 8010 Graz (Austria)
[+] These authors contributed equally to this work.

Supporting information for this article is available on the WWW under https://doi.org/10.1002/cptc.202200108

An invited contribution to the "GDCh and ChemPhotoChem: 5-Year Anniversary" Special Collection

As the photoproducts of phosphorus-based initiators are mostly highly toxic[12] and the absorption is limited at higher wavelengths for acylphosphine acids, acylsilanes were investigated as an alternative.[13] With these compounds, absorptions at higher wavelengths can be achieved. The drawbacks for this substance class are the low stability in aqueous environment and the Brook rearrangement, leading to reversibly formed siloxycarbenes, which are non-reactive towards photoinitiation.[14]

Another way to synthesize PIs with a red shifted absorption was the preparation of acylstannanes.[10] Due to the central tin atom, the nπ*- transition occurs at even higher wavelengths. A special form of tin-based PIs are R_6Sn_2 species[15] that are initiating as R_3Sn radicals.

In 2008, Ganster *et al.*[16] introduced the novel substance class of acylgermanes as PIs, which has been and continues to be a great inspiration for this research field. Although Ge-based PIs are higher in price than the previously mentioned heteroatom containing PIs, numerous advantages, such as low toxicity,[17] thermal stability[18] and the important bathochromic shift outweigh the price.

Ivocerin®, a state-of-the-art PI, is a bisacylgermane (Figure 2) with a good absorption up to 470 nm, but comes with the disadvantage of tedious purification steps.[16,19]

Based on the results regarding the successful usage and the stability of tetraacylgermanes,[16] this substance class was investigated in more detail.[1,17,20] Three different synthetic pathways towards highly efficient tetraacylgermanes were envisaged by Gescheidt, Haas, Stueger *et al.* in 2017.[17] Scheme 1 shows the most successful approach that is also used to synthesize the tetraacylgermane target compounds herein. Starting with a tetrakis(trimethylsilyl)germane, an intermediary potassium germanyl species is generated using KO*t*Bu. In the second step, a previously synthesized acid fluoride is added to receive the final tetraacylgermane.[1,17]

Herein, we want to contribute to the group of tetraacylgermanes by synthesizing the already known derivative tetrakis(2-methoxybenzoyl)germane[1] (**1 a**) and the novel derivatives tetrakis(2,6-dimethoxybenzoyl)germane (**1 b**) and tetrakis(2,4,6-trimethoxybenzoyl)germane (**1 c**) as depicted in Figure 2. By adding more methoxy groups, the absorption spectra are expected to show the desired bathochromic shift and therefore enlarge C_d. Additionally, also the solubility in polar media should be improved. The introduction of *o*-methoxy groups is already reported in literature for PIs based on acylphosphine oxides.[21]

The target compounds **1 a**–**c** are characterized *via* UV/Vis absorption spectroscopy and steady-state photolysis (SSP). Their reactivity is examined with RT-FTIR photorheology. Tetrakis(4-methoxybenzoyl)germane (**2**), tetrakis(4-ethoxybenzoyl)germane (**3**), tetrakis(2-acetoxybenzoyl)germane (**4**) and state-of-the-art PI Ivocerin® were added as a reference. **1 a** can be compared to **2** as the methoxy group is placed in a different position on the benzoyl group, with the methoxy groups in *para* position of **2** showing similarity to Ivocerin®. **3**, containing ethoxy groups, was added as a comparison compound due to its better solubility in acrylic monomers. Compound **4** was included as a reference compound in the study due to the less electron donating effects of its acetoxy groups.

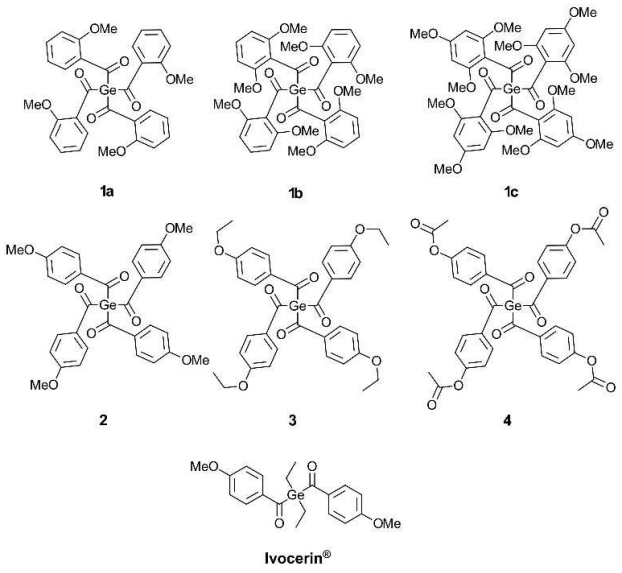

Figure 2. Structures of the target compounds **1 a**–**c** and the reference compounds **2**–**4** and Ivocerin®.

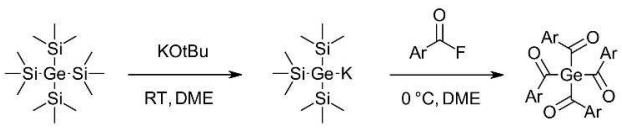

Scheme 1. Synthetic pathway towards tetraacylgermanes using tetrakis(trimethylsilyl)germane and the previously synthesized acid fluoride.[1]

Results and Discussion

Synthesis

The following syntheses of the targeted tetraacylgermanes were performed according to literature.[1,17] The tetrafunctional germanes were obtained by first reacting the tetrakis(trimethylsilyl)germane with potassium *tert*-butoxide, and subsequent reaction of the potassium germanyl species with the respective acid fluoride (see Scheme 1). Beforehand, tetrakis(trimethylsilyl)germane and the respective acid fluoride were synthesized according to literature.[22] As the performed reactions are moisture sensitive, the utilization of Schlenk techniques is necessary. The targeted compounds **1 a**–**c** were obtained as yellow powder in a yield of almost 50 % and characterized *via* NMR spectroscopy, melting point and for **1 b**–**c** HRMS measurements (see Electronic Supporting Information). The reference substances **2**–**4** were synthesized as described previously.[17]

UV/Vis Absorption Spectroscopy

When comparing the absorption spectra of the *ortho*-methoxy substituted tetraacylgermanes **1 a–c** shown in Figure 3, a higher molar extinction coefficient (ε) at the respective maximum is observed with increasing amount of methoxy groups ($\varepsilon_{max\ 1a}$ (992) < $\varepsilon_{max\ 1b}$ (1400) < $\varepsilon_{max\ 1c}$ (1930), listed in Table 2).

However, the enhanced ε is not observed in the tail out region at 460 nm. When comparing said regions, **1 a–c** show a higher absorption than all of the compared compounds. One hypothesis for the latter phenomenon, which is also stated by Gescheidt, Haas, Stueger *et al.*[1] for the alkyl substituted compounds, could be that the *ortho* substitutions are reducing the symmetry within the molecule, and thus providing more fine structures.

Steady-State Photolysis

The often undesired discoloration of a polymer, especially for esthetical applications (*e.g.* dental materials), is mainly due to the PI, as it is causing a yellowish tint. In order to obtain a colorless polymer, one important feature of a PI is the photodecomposition of its chromophores. Thus, this so-called photobleaching has to be investigated. One approach to do so is to conduct steady-state photolysis (SSP) experiments.[20,23] Here, the PI is dissolved in a suitable solvent and irradiated with a specific LED (385 nm and 460 nm) under inert conditions.

The rate of decomposition (R_d) was calculated according to literature [Equation (1)].[10,24] The value A_0 was taken from the absorbance maximum before the measurement was started, while A_1 was the value corresponding to the sample taken after 60 s (t_1) of irradiation and A_2 equals the absorbance of the sample taken after 180 s (t_2). All A values were measured at the respective λ_{max}.

$$R_d = -\frac{d[PI]}{dt} = \left(\frac{A_1 - A_2}{A_0}\right)\left(\frac{[PI]}{t_1 - t_2}\right) \quad (1)$$

All seven PIs show photobleaching whilst irradiating with 385 nm (Table 1), where the performance of Ivocerin® excels, which is also reflected in R_d. Comparing the R_d of the *ortho*-methoxy substituted compounds **1 a–c**, a higher $\varepsilon_{385\ nm}$ seems to favor fast degradation at 385 nm. The inverse behavior is observed for the decomposition behavior of the *para*-substituted tetraacylgermanes **2**–**4**. A higher R_d is obtained for derivatives with lower $\varepsilon_{385\ nm}$, as the acetoxy substituted **4** bleaches faster than the *para*-methoxy substituted **2** and

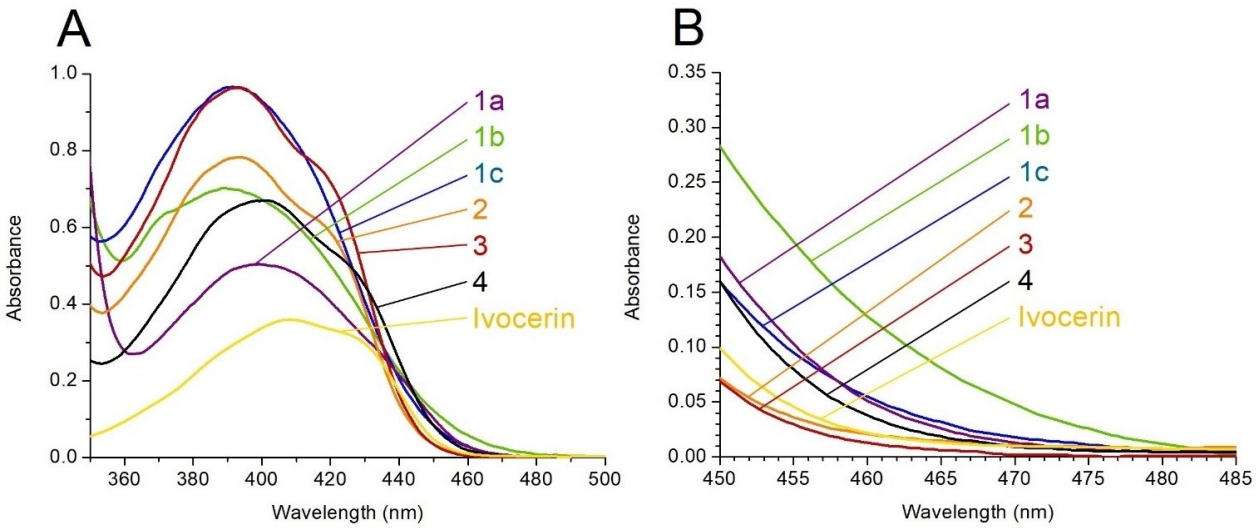

Figure 3. UV/Vis absorption spectra of the depicted tetraacylgermanes and Ivocerin®: A) concentration of measured compounds in acetonitrile $5 \cdot 10^{-4}$ M; B) expanded portion of the spectra showing the tail region - concentration of the compounds 10^{-3} M for better visibility.

Table 1. Rates of decomposition, quantum yields and extinction coefficients whilst irradiated with 385 nm and 460 nm determined using SSP experiments.

Compound	385 nm $\varepsilon_{385\ nm}$ [L mol^{-1} cm^{-1}]	$R_d \cdot 10^9$ [mol s^{-1} L^{-1}]	Φ_d [ ]	460 nm $\varepsilon_{460\ nm}$ [L mol^{-1} cm^{-1}]	$R_d \cdot 10^9$ [mol s^{-1} L^{-1}]	Φ_d
Ivocerin®	505	880	0.83[20]	22	600	0.47
1 a	878	320	0.30	57	260	0.20
1 b	1380	360	0.34	113	540	0.42
1 c	1870	370	0.34	58	230	0.17
2	1490	440	0.41	19	110	0.09
3	1830	210	0.20	14	280	0.22
4	1200	840	0.79	47	530	0.42

ethoxy substituted **3**. The increasing R_d at lower $\varepsilon_{385\,nm}$ may be explained by a higher penetration depth of light into the solution, as a low $\varepsilon_{385\,nm}$ prevents shielding.

At 460 nm, a high $\varepsilon_{460\,nm}$ seems to generally favor a high R_d for the methoxy substituted derivatives **1 a–c** and **2**. Although $\varepsilon_{460\,nm}$ of **1 a** and **1 c** are fairly similar, the difference in R_d is more prominent, favoring **1 a**. The outstanding bleaching of the dimethoxy substituted **1 b** could be explained by the better overlap with the 460 nm LED emission band, as the tail out is more pronounced. When comparing **2** with the *para*-substituted compound **3**, the latter shows a higher R_d, although $\varepsilon_{460\,nm}$ of **3** is lower than $\varepsilon_{460\,nm}$ of **2**. Here, the lower $\varepsilon_{460\,nm}$ may favor the penetration depth of light, resulting in higher amount of cleavage. The *para*-acetoxy substituted **4** shows once more outstanding photobleaching when compared to the other tetraacylgermanes. In general R_d is higher for all PIs when irradiating with 385 nm, with the exemption of **1 b** and **3**. The higher R_d of **1 b** and **3** at 460 nm could be caused by electronic effects of the benzoylic substitution pattern, facilitating the n-π^* transition, and subsequent formation of free radicals.

In order to determine the quantum yield of decomposition (Φ_d) for the measurements conducted at 385 nm, the literature[20] known $\Phi_{d\ 385\,nm}$ of Ivocerin® (0.83) was used to determine the photon flux (I_0) in the system, by transforming Equation (2):[10]

$$\Phi_d = \frac{R_d}{I_0} \tag{2}$$

After obtaining I_0 ($1.06 \cdot 10^{-6}$ mol L^{-1} s^{-1}), Φ_d was calculated for the measurements performed at 385 nm.

For the experiments performed at 460 nm, I_0 had to be determined beforehand. To the best of our knowledge, $\Phi_{d\,460\,nm}$ was not reported in literature for any of the tested PIs, making the above described procedure not applicable. Hence, a different approach for calculating I_0 was considered. By taking the wavelength λ (m), the radiation power of the LED P_{LED} (W), the Planck constant h ($6.63 \cdot 10^{-34}$ J s), the speed of light c (299 792 458 m s^{-1}), the Avogadro constant N_A ($6.02 \cdot 10^{23}$ mol^{-1}) and the reaction volume V (here 0.0385 L, as irradiation started after the removal of 1.5 mL), I_0 is generally accessible with the following Equation (3):[23]

$$I_0 = \frac{\lambda P_{LED}}{hcN_A V} \tag{3}$$

As the 385 nm and the 460 nm LED were both calibrated to 100 mW cm^{-2} after the quartz window, the assumption was made that P_{LED} is identical for both LED set-ups. By taking the calculated I_0 ($1.06 \cdot 10^{-6}$ mol L^{-1} s^{-1}) of the 385 nm LED measurements from Equation 2, and transforming Equation 3, P_{LED} was obtained ($1.27 \cdot 10^{-2}$ W). By incorporating the calculated P_{LED} and λ (460 nm) into Equation 3, the photon flux was obtained for 460 nm ($I_0 = 1.27 \cdot 10^{-6}$ mol L^{-1} s^{-1}). Hence, Φ_d of the measurements conducted with the 460 nm LED could be calculated according to Equation 2.

The results of the SSP experiments containing ε, R_d and Φ_d at each 385 and 460 nm are listed in Table 1 (all spectra are provided in the Electronic Supporting Information).

In summary, nearly all measured PIs show good photobleaching when irradiated with 385 nm, except of **3**, and 460 nm, except of **2**. Comparing the *ortho*-methoxy derivatives **1 a–c** with each other, a higher $\varepsilon_{385\,nm}$ seems advantageous for faster bleaching.

SSP conducted whilst irradiating with a 460 nm LED seems to indicate that a higher absorbance could be beneficial for a higher Φ_d for methoxy substituted tetraacylgermanes (**2**, **1 a–c**). For **1 a/1 c** and **2/3**, faster photobleaching is obtained for **1 a** and **3**, which respectively show lower absorption at 460 nm.

At both wavelengths, the acetoxy substituted **4** still showed outstanding bleaching behavior when compared with the other tetraacylgermanes, which suggests that the cleavage behavior is more likely influenced by electronic effects, favorable for radical formation, than by its absorption coefficient. At 460 nm, the dimethoxy-substituted **1 b** shows remarkable fast bleaching when compared to the other tetraacylgermanes (with exception to aforementioned **4**), which may be explained due to its more pronounced tail out, and thus better overlap with the 460 nm LED.

Table 2. Absorption maxima with the corresponding molar extinction coefficients and the molar extinction coefficients at 460 nm of the tetraacylgermanes **1 a–c**, **2–4** and Ivocerin®.

Compound	λ_{max} [nm] (ε [L mol^{-1} cm^{-1}])	$\varepsilon_{460\,nm}$ [L mol^{-1} cm^{-1}]
Ivocerin®	408 (711)	22
1 a	399 (992)	57
1 b	389 (1400)	113
1 c	392 (1930)	58
2	393 (1550)	19
3	394 (1900)	14
4	401 (1340)	47

RT-FTIR Photorheology

A facile method for testing the photoreactivity of a monomer-initiator system is the utilization of a real-time Fourier transform infrared spectroscopy photorheometer (RT-FTIR photorheometer). This device is composed of a rheometer, a light source (here LED), which irradiates the sample during measurement, and a real time near infrared spectrometer to obtain chemical data simultaneously with the mechanical information. The set-up and the schematic depiction of gained information is shown in Figure 4.[25] With this set-up, the double bond conversion (DBC) as well as the time to reach 95 % of the DBC (t_{95}) and the rate of polymerization (R_p) were investigated.

Hexanediol diacrylate (HDDA), being a very common monomer in photopolymer applications, has been chosen to prepare the formulations for photorheology measurements. Here, compounds **2** and **4** were found to be insoluble in comparison to **3**, which could be dissolved more easily. Hence,

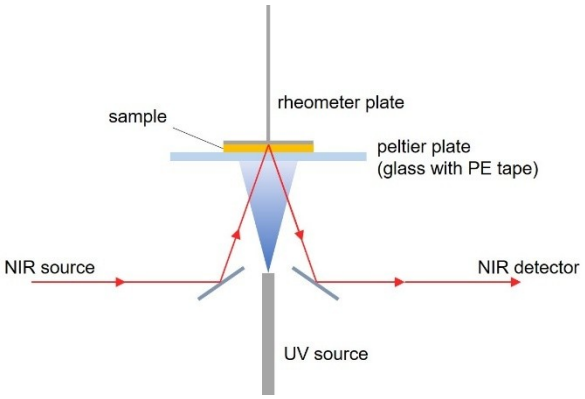

Figure 4. Schematic depiction of the RT-FTIR photorheometer.

only compounds **1 a**–**c**, **3** and Ivocerin® were used in these formulations (the exact composition can be found in the Electronic Supporting Information). As Ivocerin® is releasing only half of the radicals during initiation (compared to the tetraacylgermane derivatives) a formulation with double the concentration was also investigated (2× Ivocerin®) to enable an unbiased discussion.

Figure 5 shows a typical diagram of the DBC during the photorheology measurements of 2× Ivocerin® and **1 b** at 460 nm with a steep increase at the first seconds of the experiments and a steadily flattening progress afterwards. The final DBC was reached at the very end of the measurements and therefore calculated from the DBC measured between 300 and 317 s (grey marked area). For better visualization, the final DBC was highlighted as dashed lines in the corresponding color of the PI. The biggest difference between the components is the t_{95} value, marked in orange and dark blue in Figure 5. R_p was calculated from the steep slope measured in the first seconds of the experiments. A diagram with the rheological data for the same measurements can be found in the Electronic Supporting Information. The summarized results including the DBC, t_{95} and R_p are displayed in Table 3 and Table 4, respectively.

The reactivities of the tested PIs in HDDA are fairly similar when irradiated with a 385 nm LED with respect to DBC and t_{95}. Although the R_p are more diverse, no evident connection could be made in regards to the photobleaching behavior (R_d and Φ_d).

The results obtained from the measurements conducted at 460 nm showed to be more different, in such that t_{95} reveals the smallest value for **1 a**, and the biggest value for **3**. When comparing the initiation behavior, the dimethoxy substituted **1 b** (with the highest $R_{p\,460\,nm}$ in the measurement series) excels, as it is the only tetraacylgermane outperforming the double molar amount of Ivocerin® whilst irradiated with 460 nm.

Conclusion

In summary, the novel compounds **1 b** and **1 c** were synthesized successfully and characterized *via* NMR spectroscopy, UV/Vis absorption spectroscopy, melting point and HRMS measurements.

UV/Vis absorption spectroscopy revealed the increasing ε value at λ_{max} from **1 a**–**c**, related to the increasing number of methoxy groups. Additionally, **1 b** and **1 c** show the highest $\varepsilon_{460\,nm}$ compared to the tetraacylgermanes **1 a**, **2**–**4** and Ivocerin®, which is highly desirable for enhancing the penetration depth of light in the curable formulation due to a bathochromic shift.

SSP experiments were conducted at 385 and 460 nm, respectively, for investigating the photobleaching behavior. **1 b** and **4** showed outstanding properties especially when irradiated with 460 nm with only Ivocerin® performing slightly better.

The reactivity of Ivocerin®, **1 a**–**c** and **3** in HDDA was investigated *via* RT-FTIR photorheology, where at 385 nm **1 a**–**c**

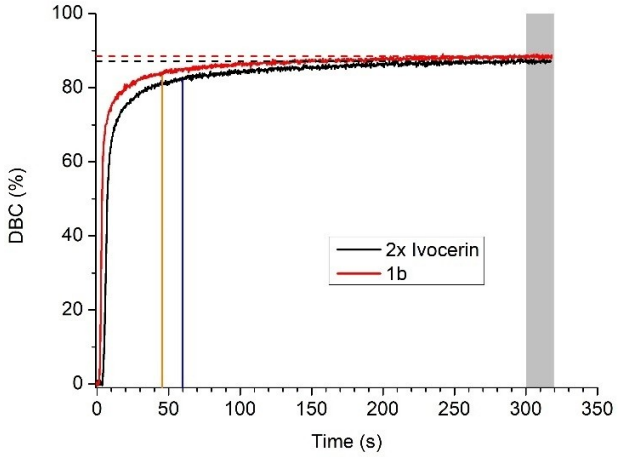

Figure 5. DBC diagram of the photorheology experiments with 2× Ivocerin® and **1 b** at 460 nm. Final DBC of the measurements are marked with the dashed lines as an average from the grey area, t_{95} is marked as an orange line for **1 b** and as a dark blue line for 2× Ivocerin®.

Table 3. Results of the photorheological measurements of the HDDA mixtures at 385 nm. Φ_d was obtained by steady-state photolysis.

PI	$\Phi_{d\,385\,nm}$	DBC [%]	t_{95} [s]	R_p [% s^{-1}]
Ivocerin®	0.83 (lit. [20])	88.4 ± 0.8	31.3 ± 2.8	53.4 ± 4.0
2× Ivocerin®	–	90.6 ± 0.6	25.2 ± 2.7	67.9 ± 2.7
1 a	0.30	89.0 ± 0.1	27.9 ± 1.1	65.2 ± 4.1
1 b	0.34	88.8 ± 0.1	27.5 ± 1.3	67.8 ± 3.8
1 c	0.34	89.2 ± 0.1	27.4 ± 3.0	73.4 ± 5.6
3	0.20	89.7 ± 0.1	28.0 ± 1.1	74.5 ± 3.5

Table 4. Results of the photorheological measurement of the HDDA mixtures at 460 nm. Φ_d was obtained by steady-state photolysis.

PI	$\Phi_{d\,460\,nm}$	DBC [%]	t_{95} [s]	R_p [% s^{-1}]
Ivocerin®	0.47	86.9 ± 0.3	60.2 ± 0.6	18.2 ± 0.4
2× Ivocerin®	–	88.8 ± 0.2	52.2 ± 1.7	25.5 ± 0.3
1 a	0.20	89.7 ± 0.5	37.0 ± 6.7	24.2 ± 3.0
1 b	0.42	88.7 ± 0.4	42.9 ± 1.7	30.3 ± 1.3
1 c	0.17	87.9 ± 0.1	57.0 ± 3.9	23.6 ± 0.4
3	0.22	86.1 ± 0.2	73.8 ± 2.0	16.2 ± 0.6

performed similar to Ivocerin®. In experiments at 460 nm, **1 b** outperformed the comparison compounds in reactivity with the highest R_p. Due to the increase of methoxy groups, **1 a–c** showed higher solubility in HDDA than the PIs **2** and **4**, which could not be dissolved under any circumstances.

In conclusion, tetraacylgermanes exhibit sufficient reactivity towards acrylates and the desired red shift in their absorption spectra especially in the tail out region from 450 to 480 nm, as required for LCM. Compound **1 b** in particular was established as a promising PI for future applications as a potential alternative to Ivocerin® as the state-of-the-art PI.

Experimental Section

Materials and Equipment

All reagents and solvents were purchased from Sigma Aldrich®, TCI®, abcr GmbH®, VWR®, Isovolta® and Ivoclar Vivadent®, and, unless stated otherwise, used as received. Anhydrous solvents were either used as received or taken from a PURESOLV™-plant from Innovative technology®. Tetrakis(4-methoxybenzoyl)germane (**2**), tetrakis(4-ethoxybenzoyl)germane (**3**) and tetrakis(4-acetoxybenzoyl)germane (**4**) were synthesized as described previously.[17] Tetrakis(trimethylsilyl)germane and the corresponding acid fluorides were prepared prior according to literature.

^{1}H-NMR, ^{13}C-NMR,^{19}F-NMR and ^{29}Si-NMR spectra were recorded with a Bruker® Avance DRX-400 FT-NMR, Bruker® AC-E 200-FT-NMR, NMReady-60e 60 MHz benchtop NMR (by nanalysis®), Varian® INOVA-300 NMR or Varian® Mercury 300 NMR. NMR for reaction monitoring were performed with a D_2O capillary, to gain a deuterium-lock-signal. Analysis of the spectra was carried out using a Bruker® TopSpin 3.2 or MestReNova software from Mestralab®.

The melting points of **1 a–c** were obtained using a Kofler hot-stage microscope with a heating rate of 1–3 °C/min.

HRMS analysis was performed using 10 μM solutions in acetonitrile by an HTC PAL system autosampler (CTC Analytics AG, Zwingen, Switzerland), and Agilent 1100/1200 HPLC with binary pumps, degasser and column thermostat (Agilent Technologies, Waldbronn, Germany) together with an Agilent 6230 AJS ESI-TOF mass spectrometer (Agilent Technologies, Palo Alto, United States). The data was analyzed using an Agilent MassHunter Qualitative Analysis software.

Synthesis – General procedure 1 a–c

1 eq. of tetrakis(trimethylsilyl)germane and 1.1 eq. KOtBu were stirred in dry DME under inert atmosphere for 30 min and afterwards cooled to 0 °C. The corresponding acid fluoride was dissolved in dry DME and added slowly to the cooled solution protected from light below 480 nm. The mixture was stirred and warmed up to room temperature overnight. For purification, the reaction was extracted with sat. aqueous NH_4Cl solution. The aqueous phase was extracted with DCM until it was colorless. The combined organic phases were washed with water and dried over Na_2SO_4. After evaporating the solvent, the product was dried under high vacuum. The detailed procedures can be found in the Electronic Supporting Information.

UV/Vis absorption spectroscopy

Solutions of 10^{-3} mol L^{-1} were made for tetrakis(2-methoxybenzoyl)germane (**1 a**), tetrakis(2,6-dimethoxybenzoyl)germane (**1 b**), tetrakis(2,4,6-trimethoxybenzoyl)germane (**1 c**), tetrakis(4-methoxybenzoyl)germane (**2**), tetrakis(4-ethoxybenzoyl)germane (**3**) tetrakis(4-acetoxybenzoyl)germane (**4**) and Ivocerin® in acetonitrile. The solutions were prepared under exclusion of light with wavelength below 480 nm and were transferred into brown penicillin flasks. Afterwards the solutions were put into quartz cuvettes (d = 10 mm) directly before recording the spectra. In order to determine the extinction coefficient, stock solutions of 0.002 mol L^{-1} were prepared. Subsequently these solutions were diluted to obtain the concentrations C1 (1 mM), C2 (0.5 mM) and C3 (0.25 mM) for each compound. The extinction coefficients were determined from the slope of absorption (at each 385 nm and 460 nm) against the concentration with set intercept to 0. The UV vis spectra were recorded using a Thermo Scientific™ NanoDrop™ One Microvolume UV-Vis spectrometer and a PerkinElmer® Lambda900 UV/Vis/NIR spectrometer. The measurements were conducted using a PerkinElmer® Lambda 900 UV/Vis/NIR spectrometer.

Steady-state photolysis

For the SSP experiments, solutions of 10^{-3} mol L^{-1} of Ivocerin®, **1 a–c**, **2**, **3** and **4** (40 mL each) were prepared and transferred into a two neck round bottom flask equipped with a septum, a quickfit with quartz window and stirring bar. The solutions where then degassed for 20 minutes by bubbling with inert gas. The tip of the lightguide was inserted into the quickfit with quartz window on the bottom. The intensity behind the glass window was set previously to 100 mW cm^{-2} for each LED. The first sample of 1.5 mL was taken before starting the irradiation for the 0 s measurement. Then the LED (385 nm or 460 nm) was switched on for 15 minutes while stirring under inert atmosphere (argon/nitrogen). Samples of 1.5 mL each were taken after 1, 3, 6, 10 and 15 minutes and transferred undiluted into brown penicillin vials. After all samples were taken, they were subsequently transferred to quartz cuvettes (d = 10 mm) to conduct UV/Vis absorption spectroscopic measurements. The setup is described in detail in the Electronic Supporting Information.

RT-FTIR photorheology

All formulations were prepared under exclusion of light with wavelength below 480 nm. to prevent premature polymerization. Each formulation consisted of 0.17 mol% (**1 a–c**, Ivocerin®)/ 0.34 mol% (2× Ivocerin®) PI in HDDA. In order to dissolve the monomer completely, the suspensions were heated in the water bath up to 55 °C and put in the ultrasonic bath afterwards for 15 minutes. These steps were repeated until the PIs were completely dissolved. All measurements were performed at 25 °C with a gap size of 200 μm between the glass plate (plus PE tape) and the measuring plate (25 mm diameter) with a 385 nm/460 nm LED at 10 mW cm^{-2} respectively. The triplicates were conducted by transferring 150 μL of each formulation on the PE tape. To determine the DBC, FTIR spectra were recorded from 4000 cm^{-1} to 7000 cm^{-1}. The acrylate band at ~6160 cm^{-1} was integrated and plotted against time. The slope of the obtained curve was subsequently used to determine R_p. Photorheology measurements were conducted on an Anton Paar® MCR 302 WESP with a P-PTD 200/GL Peltier glass plate and a PP25 measuring system. The rheometer was coupled with a Bruker® Vertex 80 FTIR spectrometer. The rheological data was analyzed using the Anton Paar® Rheoplus software. The analysis of the FTIR-spectra was performed using the OPUS 7.0 software. For irradiating the samples, an

OmniCure® LX400 UV-LED-spot curing system was used with a 385 nm LED and 460 nm LED. In order to measure the light intensity an Ocean Optics 2000+ USB device was used with the software SpectraSuit.

Acknowledgements

Funding by the Christian Doppler Research Association (Christian Doppler Laboratory for Advanced Polymers for Biomaterials and 3D Printing), the Austrian Federal Ministry for Digital and Economic Affairs and the National Foundation for Research, Technology and Development is gratefully acknowledged. Additionally, this work was supported by Lithoz GmbH, Karl Leibinger Medizintechnik GmbH & Co. KG and Trauma Care Consult. The authors acknowledge TU Wien Bibliothek for financial support through its Open Access Funding Programme.

Conflict of Interest

The authors declare no conflict of interest.

Data Availability Statement

The data that support the findings of this study are available from the corresponding author upon reasonable request.

Keywords: ceramic manufacturing · germanium · photoinitiators · photopolymerization · radicals · rheology

[1] J. Radebner, M. Leypold, A. Eibel, J. Maier, L. Schuh, A. Torvisco, R. Fischer, N. Moszner, G. Gescheidt, H. Stueger, M. Haas, *Organometallics* **2017**, *36*, 3624–3632.
[2] K. K. Dietliker, P. Oldring, *Chemistry and Technology of UV and EB Formulation for Coatings, Inks and Paints. Photoinitiators for Free Radical and Cationic Polymerisation, Vol. 3*, SITA Technology, **1991**.
[3] T. Billiet, M. Vandenhaute, J. Schelfhout, S. Van Vlierberghe, P. Dubruel, *Biomaterials* **2012**, *33*, 6020–6041.
[4] N. Moszner, U. Salz, *Prog. Polym. Sci.* **2001**, *26*, 535–576.
[5] E. Kroll, D. Artzi, *Rapid Prototyping J.* **2011**, *17*, 393–402.
[6] J. P. Kruth, M. C. Leu, T. Nakagawa, *CIRP Ann.* **1998**, *47*, 525–540.
[7] M. Schwentenwein, P. Schneider, J. Homa, *Adv. Sci. Technol. Res. J.* **2014**, *88*, 60–64.
[8] A. A. Altun, T. Prochaska, T. Konegger, M. Schwentenwein, *Appl. Sci.* **2020**, *10*, 996.
[9] a) V. Tomeckova, J. W. Halloran, *J. Eur. Ceram. Soc.* **2010**, *30*, 2833–2840; b) G. Mitteramskogler, R. Gmeiner, R. Felzmann, S. Gruber, C. Hofstetter, J. Stampfl, J. Ebert, W. Wachter, J. Laubersheimer, *Addit. Manuf.* **2014**, *1–4*, 110–118; c) C.-J. Bae, J. W. Halloran, *Int. J. Appl. Ceram. Technol.* **2011**, *8*, 1255–1262; dJ. H. Lee, R. K. Prud'Homme, I. A. Aksay, *J. Mater. Res.* **2001**, *16*, 3536–3544.
[10] M. Mitterbauer, P. Knaack, S. Naumov, M. Markovic, A. Ovsianikov, N. Moszner, R. Liska, *Angew. Chem. Int. Ed.* **2018**, *57*, 12146–12150; *Angew. Chem.* **2018**, *130*, 12323–12327.
[11] T. Sumiyoshi, W. Schnabel, A. Henne, P. Lechtken, *Polymer* **1985**, *26*, 141–146.
[12] U. Kolczak, G. Rist, K. Dietliker, J. Wirz, *J. Am. Chem. Soc.* **1996**, *118*, 6477–6489.
[13] M. Mitterbauer, M. Haas, H. Stüger, N. Moszner, R. Liska, *Macromol. Mater. Eng.* **2017**, *302*, 1600536.
[14] J. M. Duff, A. G. Brook, *Can. J. Chem.* **1973**, *51*, 2869–2883.
[15] J.-S. Kim, A. Dutta, V. Vasu, O. I. Adebolu, A. D. Asandei, *Macromolecules* **2019**, *52*, 8895–8909.
[16] B. Ganster, U. K. Fischer, N. Moszner, R. Liska, *Macromolecules* **2008**, *41*, 2394–2400.
[17] J. Radebner, A. Eibel, M. Leypold, C. Gorsche, L. Schuh, R. Fischer, A. Torvisco, D. Neshchadin, R. Geier, N. Moszner, R. Liska, G. Gescheidt, M. Haas, H. Stueger, *Angew. Chem. Int. Ed.* **2017**, *56*, 3103–3107; *Angew. Chem.* **2017**, *129*, 3150–3154.
[18] J. Radebner, PhD thesis, Graz University of Technology (Graz), **2018**.
[19] M. Haas, J. Radebner, A. Eibel, G. Gescheidt, H. Stueger, *Chem. Eur. J.* **2018**, *24*, 8258–8267.
[20] A. Eibel, J. Radebner, M. Haas, D. E. Fast, H. Freißmuth, E. Stadler, P. Faschauner, A. Torvisco, I. Lamparth, N. Moszner, *Polym. Chem.* **2018**, *9*, 38–47.
[21] C. Dietlin, T. T. Trinh, S. Schweizer, B. Graff, F. Morlet-Savary, P.-A. Noirot, J. Lalevée, *Macromolecules* **2019**, *52*, 7886–7893.
[22] a) C. Kaduk, H. Wenschuh, M. Beyermann, K. Forner, L. A. Carpino, M. Bienert, *Lett. Pept. Sci.* **1996**, *2*, 285–288; b) J. B. Baell, P. J. Duggan, S. A. Forsyth, R. J. Lewis, Y. Phei Lok, C. I. Schroeder, *Bioorg. Med. Chem.* **2004**, *12*, 4025–4037; c) A. G. Brook, F. Abdesaken, H. Söllradl, *J. Organomet. Chem.* **1986**, *299*, 9–13.
[23] E. Stadler, A. Eibel, D. Fast, H. Freißmuth, C. Holly, M. Wiech, N. Moszner, G. Gescheidt, *Photochem. Photobiol. Sci.* **2018**, *17*, 660–669.
[24] J.-P. Fouassier, J. F. Rabek, in *Radiation curing in polymer science and technology: Fundamentals and methods, Vol. 1*, Springer Science & Business Media, **1993**.
[25] C. Gorsche, R. Harikrishna, S. Baudis, P. Knaack, B. Husar, J. Laeuger, H. Hoffmann, R. Liska, *Anal. Chem.* **2017**, *89*, 4958–4968.

Manuscript received: April 12, 2022
Revised manuscript received: July 13, 2022
Accepted manuscript online: July 19, 2022
Version of record online: ■■, ■■■

RESEARCH ARTICLES